Analysis of Surface Current Response to Wind

A. D. KIRWAN, JR.

Texas A&M University, Department of Oceanography, College Station 77843

G. MCNALLY, S. PAZAN AND R. WERT

Scripps Institution of Oceanography, La Jolla, CA 92093

(Manuscript received 12 May 1978, in final form 17 October 1978)

ABSTRACT

The response of the surface current to the wind has been described at various times by quadratic and linear laws. The quadratic response leads to Ekman-type currents while the linear response may be indicative of Stokes drift. The velocity records of six satellite-tracked drifters which lost their drogues and the Fleet Numerical Weather Central's surface wind analysis were used to test the relative merits of these responses. It was concluded that a linear law relating the wind and the wind drift surface current was superior to the classic quadratic law. The angle between the wind and the surface current predicted by the model was about 15° *cum sole*. However, it was also found that a model which superposed the Ekman quadratic response and linear Stokes drift response explained the data just as well as the linear law.

1. Introduction

The surface-layer response of the ocean to the surface wind has been a fundamental problem in ocean dynamics ever since Ekman's (1905) pioneering study. That model employed a constant eddy viscosity and assumed a velocity discontinuity at the air-sea interface. It predicted that surface wind drift currents move 45° *cum sole* to the wind.

The extensive literature on the subject indicates a widespread uneasiness with this explanation of the surface-layer response. As a result, the simple Ekman model has been extended to include variable eddy viscosities as well as boundary layers on either side of the air-sea interface. In these studies the angle between the wind drift current and the wind is determined by the boundary-layer parameters. Madsen (1977) has given a lucid analysis along these lines as well as a review of previous results.

An alternate response mechanism has been suggested by Longuet-Higgins (1969), Kenyon (1969) and Ianniello and Garvine (1975) who noted that much of the wind energy gets into the ocean through wave generation. The nonlinear character of the waves would then induce a Stokes drift which could be comparable to geostrophic or wind drift currents. The Coriolis acceleration acting on this wave drift, however, in the steady state is exactly balanced by an Eulerian transport (Hasselmann, 1970).

Resolving wind and wave-drift components from each other and from a larger scale main flow is a formidable experimental problem. Most laboratory and field investigations have focused on just one component. A notable exception has been the study of Lange and Hühnerfuss (1978). There the combined drift response in a wind-wave tunnel and a tidal estuary was observed by monomolecular slicks. The observations were in good agreement with other studies but because of the limited time and space scales and the fact that the films drastically dampen capillary waves they may not be representative of mid-ocean conditions.

The study of Davis *et al.* (1978) is more indicative of such conditions. They found the lower frequency currents nearly parallel in the upper 135 m of the ocean. Furthermore, the observed wind drift transport was five times the theoretical Ekman transport and essentially parallel to the wind. It is doubtful that their data contained a significant Stokes drift as the observed winds were light, but it was not clear whether the same was true for a geostrophic component.

In October 1975 we deployed six drifters in the eastern North Pacific. They were tracked remotely by the Random Access Measurement System (RAMS) onboard Nimbus 6. Kirwan *et al.* (1976) have provided a summary of how this system works. The main goal of the deployment was to examine the large-scale, quasi-geostrophic, surface-layer circulation in the North Pacific. To this end, the drifters were drogued at 35 m by 9.2 m parachutes.

Unfortunately, very early in the deployment the

0022-3670/79/020401-12$07.00
© 1979 American Meteorological Society

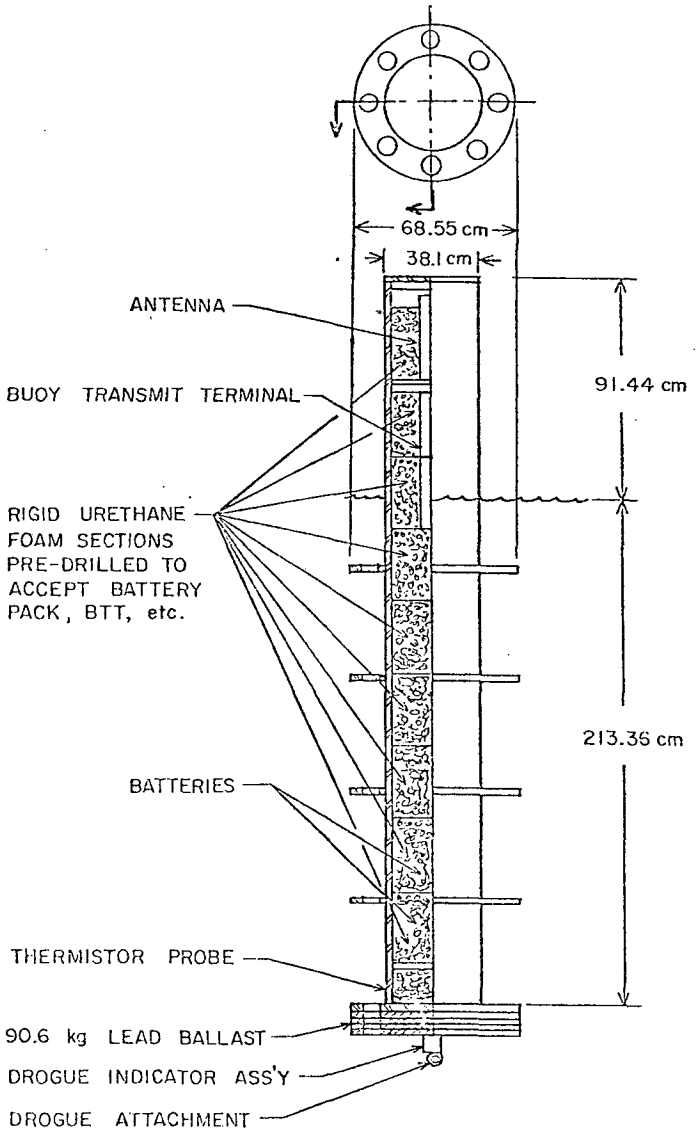

FIG. 1. Line drawing of buoy hull used in this study.

parachutes fell off. (Engineering analysis has determined the cause of this failure; it has been rectified in subsequent deployments.) According to Kirwan *et al.* (1975), drifters without drogues could respond mostly to wind forcing if the area exposed to the air was not suitably smaller than the subsurface area. Because of that study, buoy hulls with much less wind resistance were used here (see Fig. 1).

Without drogues, the drifters' motions are a combination of wind and surface-current drag (which also is a function of the wind). As explained elsewhere (Kirwan *et al.*, 1978a), an attempt was made to correct the drifter velocity for the wind drag on the exposed part of the hull. It was found that the "corrected" surface velocity vectors were unrealistic. The discrepancies in azimuth and magnitude were so large that the approach suggested by Kirwan *et al.* (1975) for estimating windage for the buoy used there is questionable. Hence, the uncorrected drifter velocities are taken to be the best representation of the surface currents available for this study. As such they are pertinent to the question of the nature of the response of ocean currents to the wind.

Three possibilities for this response have been proposed. In the classic theory, the wind drift surface current is a function of the product of the wind magnitude and the vector wind. In this theory the shear stress is continuous across the air-sea interface but the velocity is not. We call this the quadratic theory. On the other hand, Neumann and Pierson (1966) and Lange and Hühnerfuss (1978) cited a number of studies in which the surface wind

drift current and the wind are empirically linearly related. Theoretically a linear relation can arise from matching turbulent boundary layers on either side of the interface or from Stokes drift. Finally the linear and the quadratic responses are superposed to form what is called here the Ekman plus Stokes theory. This name was selected because the Lagrangian nature of the observations is particularly suited for observing Stokes drift.

The drifter data, along with estimates of the surface wind, are used here to test quantitatively some mechanisms for surface-layer response to the wind. Specifically, the following hypotheses are examined:

1) The wind drift surface current magnitude is a function of the surface wind speed squared as predicted by Ekman theory.

2) The "Ekman" angle of 45° is the best relation between the surface wind and the surface wind drift current.

3) Stokes drift is not a major component of the surface circulation.

The first two hypotheses test aspects in which the Ekman and recent boundary layer theories disagree. The last hypothesis addresses the question of the importance of Stokes drift in the wind response. The drifter data are particularly well suited for testing this hypothesis as Stokes drift is a process seen only by drifters.

The two sources of data for the study are the velocities obtained from the drifter trajectories and the Fleet Numerical Weather Central (FNWC) surface wind objective analysis. The trajectories of the six drifters used in the study are discussed by Kirwan *et al.* (1978a). Briefly, one drifter (ID1275) was launched south of the subtropical front at 30° N, 158° W. North of the front ID's 1102 and 1204 were launched at 34° N, 158° W and ID's 1173, 1232 and 1243 were launched at 36° N, 158° W. The trajectories all show eastward flow with considerable mesoscale structure. The wind field evaluated at the drifters is shown in Fig. 2. This stick diagram also summarizes the calculations discussed below. Focusing on just the winds and observed currents the overall impression is that during steady wind periods the drifter velocities are generally to the right of the wind. Fig. 3 presents composite histograms of the wind azimuth, observed drifter azimuth and their difference for all six drifters. It is seen from this figure that on the average the drifter velocity is 25°–30° to the right of the wind with a standard deviation of 15°. The drifter azimuth, however, includes both wind-driven and geostrophic components.

2. Errors in data fields

To the authors' knowledge, the most definitive test of the FNWC surface analysis was performed by Friehe and Pazan (1978). In that study the surface analysis was compared with observations from the *Alpha* buoy moored at 35° N, 155° W. The FNWC analysis was made without the incorporation of *Alpha* buoy data. The comparison was made for 60 days and indicated excellent agreement. However, any errors in the FNWC surface wind analyses obviously have an adverse effect on the ability of the models tested here to explain even more variance than they do. The Friehe and Pazan results are too limited to quantify adequately the effects of errors in the wind field on our calculations and thus, we have not included this effect in our analysis.

There are two sources of error in the drifter data. The first arises because the frequency and accuracy of the position determination does not adequately resolve small-time and space-scale motions of the ocean. This has been investigated in some detail by Kirwan and Chang (1979). Application of the results of that study show that space scales of the order of 5 km and time scales of the order of 12 h or less could not be resolved by these data. These considerations along with the Gaussian nature of the position errors have led to a smoothing/interpolation routine which produces velocity estimate with a theoretical standard deviation of 0.02 ms^{-1}.

The other error source in the drifter data is a motion produced by the wind drag on the buoy. As mentioned above, Kirwan *et al.* (1978a) have examined this effect and concluded that a windage correction did not yield realistic results as the corrected velocities at high wind speeds were much larger than the observed drifter velocities as well as being opposed to the winds.

In addition to the different observation errors associated with the wind and drifter data sets, there is an intrinsic difference in their statistics. In the former data set considerable spatial smoothing may suppress much of the natural variability. However, this is not true for the raw drifter data. When such data sets are compared, the estimated correlations generally are lower than the true. Corrective procedures are available for such a situation. These require knowledge of the response characteristics of the smoothing operators. As this is not known for the wind data we were forced to abandon this approach. But, as noted below, some of this effect is removed by the interpolation procedure.

3. Analysis procedure

Neglecting horizontal velocity variations and assuming steady-state conditions, the equations of motion reduce to

$$(K\mathbf{W}'') + (\mathbf{f} \times \mathbf{W})_H = 0, \qquad (1)$$

where K is the vertical eddy viscosity, $\mathbf{W}$ represents the difference between the actual velocity and the

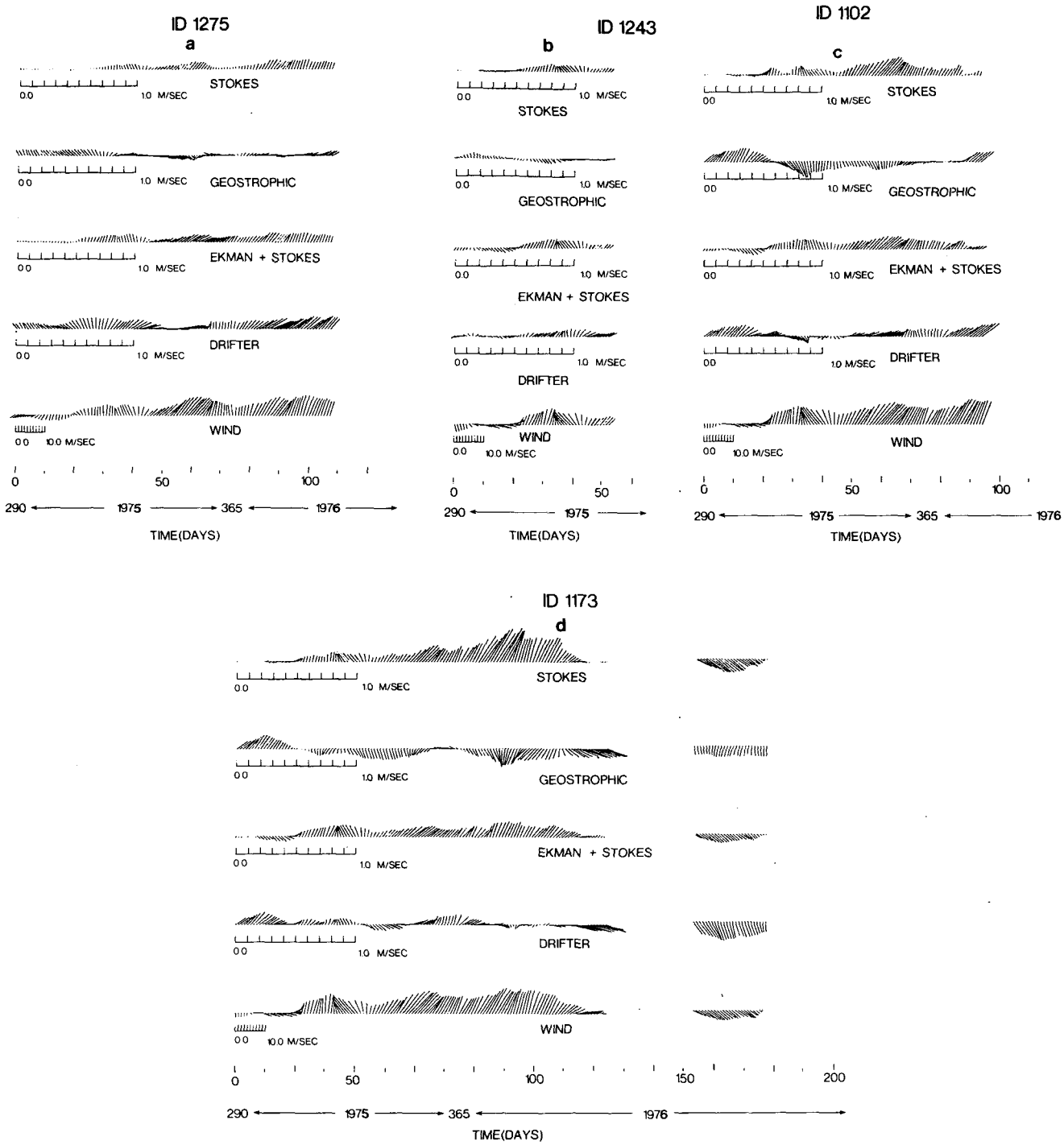

FIG. 2. Stick diagrams of observed wind at 19.5 m, observed drifter velocity and the component velocities of the Ekman plus Stokes case 2 model. Drifter ID 1275 (a) was deployed at 30° N, 158° W; ID's 1243 and 1102 (b,c) were deployed at 34° N, 158° W; and ID's 1173, 1204 and 1232 (d,e,f) were deployed at 36° N, 158° W. The gap in the records is the result of missing wind data at FNWC.

geostrophic component, the prime means differentiation with respect to the vertical coordinate Z and $(\mathbf{f} \times \mathbf{W})_H$ is the horizontal component of the Coriolis acceleration. The solution to (1) is well known and is composed of a wind drift velocity which decays exponentially with depth and a geostrophic velocity. As the observations are Lagrangian, there is the possibility that Stokes drift is also significant. Thus,

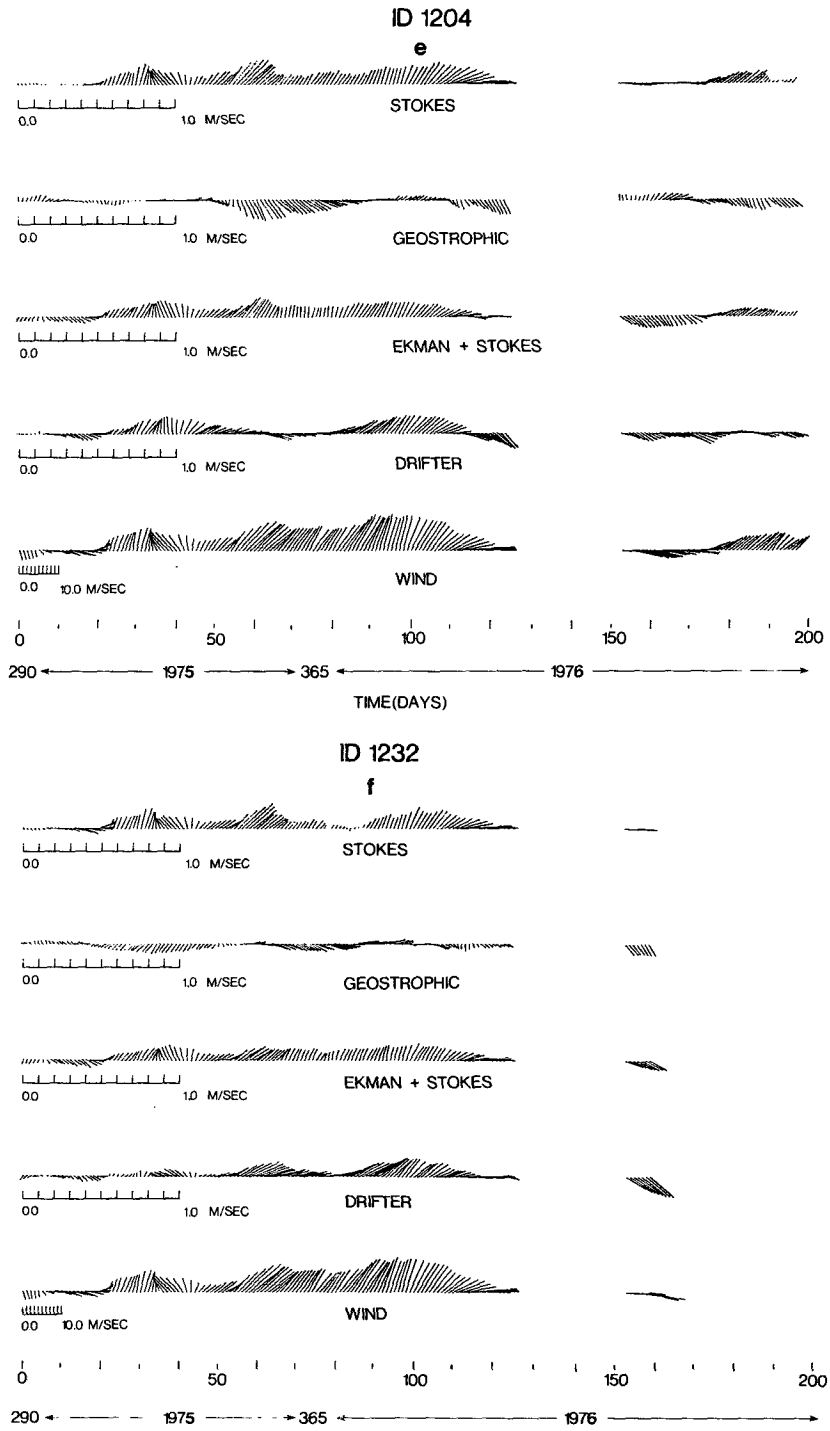

FIG. 2. *(Continued)*

at the surface the solution can be expressed as

$$\mathbf{V} = \mathbf{W} + \mathbf{V}_G = \mathbf{V}_G + \mathbf{V}_E + \mathbf{V}_S. \tag{2}$$

The subscripts denote the appropriate components. The specific form depends on the boundary conditions employed and the dependency of K and $\mathbf{V}_G$ on Z.

An expression for the Stokes drift for a random, unidirectional, fully developed sea was first given by Chang (1969). She showed that at the surface the Stokes drift is given by

$$\mathbf{V}_S = 2\int_0^\infty \frac{\sigma^3}{g}\,\mathbf{S}(\sigma)d\sigma. \tag{3}$$

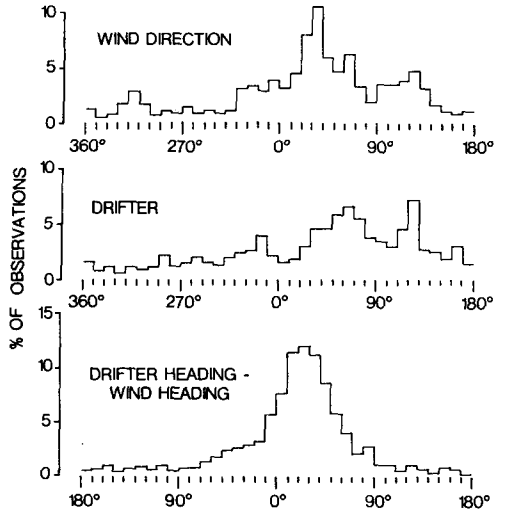

FIG. 3. Composite histogram for all six drifters of wind direction, drifter heading and the drifter heading less the wind direction. The directions are true relative to north.

Because of its analytic simplicity, we have elected to use the Pierson-Moskowitz (1964) spectral form for $S(\sigma)$ for a fully developed sea.

Inserting this spectrum into (3) gives

$$\mathbf{V}_S = \frac{\alpha\Gamma(1/4)}{2\beta^{1/4}}\,\mathbf{V}_a, \tag{4}$$

where $\mathbf{V}_a$ is the surface (19.5 m) wind. Recent experimental evidence (Barnett and Kenyon, 1975) shows the nondimensional constants α and β to be, respectively,

$$\alpha = 8.1 \times 10^{-3},\quad \beta = 0.74.$$

This then yields a theoretical Stokes drift of

$$\mathbf{V}_S = 0.0158\,\mathbf{V}_a. \tag{5}$$

The estimates of the surface current from the drifters and the surface wind from FNWC make it possible to test the hypotheses stated in Section 2 by least-squares methods. However, the errors in the data sets will adversely affect the correlations between the different fields. Thus, there is a need for an *ad hoc* standard for the maximum amount of variance that can be explained by each theory. For the quadratic and linear theories, the most general empirical form of the respective law is used as this indicator. The general form becomes the standard for objective tests of the relative effectiveness of each special case for that particular theory.

Specifically, the standard statistical model for the quadratic and linear theories takes the form

$$\left.\begin{aligned} U &= U_G + a_{11}F_1(U_a,V_a) + a_{12}F_2(U_a,V_a)\\ V &= V_G + a_{21}F_1(U_a,V_a) + a_{22}F_2(U_a,V_a)\end{aligned}\right\}. \tag{6}$$

The form for F_1 and F_2 depends on which theory is specified. For the quadratic law

$$F_1 = M_a U_a,$$
$$F_2 = M_a V_a,$$
$$M_a = (U_a^2 + V_a^2)^{1/2},$$

and for the linear law

$$F_1 = U_a,$$
$$F_2 = V_a.$$

The U_G, V_G and a_{ij}'s are computed by least squares. As the coefficients appear in a vector equation, two regression equations must be solved. Not only are the disturbance terms in the two equations correlated but as indicated below in some of the calculations constraints imposed on the coefficients couple the equations directly. Indirect and multistage least squares as well as maximum likelihood techniques are frequently used in these situations, usually at great computational cost. We have elected instead to use ordinary least squares to minimize the mean square scalar residual as the means for calculating U_G, V_G and the a_{ij}'s. This procedure, which is an obvious extension of the familiar single equation regression, has the advantages that standard F tests can be used to establish levels of significance for the constrained cases and that there is considerable computational simplicity. The price of these advantages is that ordinary least squares does not explain the maximum amount of variance. More sophisticated regression techniques combined with better quality data no doubt would increase the levels of significance of the hypothesis tests, but presumably would not affect our conclusions.

For the quadratic and linear theories the following three cases were investigated. The first was the general case in which each of the a_{ij}'s were taken as independent. This established the maximum amount of variance that could be explained by that theory. Physically this case allowed for an arbitrary angle between the wind and wind drift surface current as well as different drag coefficients for the east and north directions. The second case allowed for only one drag coefficient and an arbitrary angle. This was accomplished by imposing the constraints $a_{11} = a_{22}$ and $a_{12} = -a_{21}$. The final case fixed the angle at 45° *cum sole*. This required the constraints $a_{11} = a_{12} = a_{22} = -a_{21}$. In this case only a drag coefficient was determined.

For the general cases the U_G, V_G and the a_{ij}'s are found by minimizing

$$\overline{E^2} = \overline{(\mathbf{V}_D - \mathbf{V})\cdot(\mathbf{V}_D - \mathbf{V})}. \tag{7}$$

Here $\mathbf{V}_D$ is the observed drifter velocity vector. The overbar means a time average. For the constrained cases (7) was modified by the method of Lagrangian multipliers.

In order to assess wave drift an Ekman plus Stokes theory was assumed. This was a superposition of wind and wave drift. For this theory (7) was replaced by

$$\overline{E^2} = \overline{(\mathbf{V}_D - \mathbf{V} - \mathbf{V}_S)\cdot(\mathbf{V}_D - \mathbf{V} - \mathbf{V}_S)}. \quad (8)$$

Rather than use the theoretical value of the coefficient as given by (5) a general form of V_S was used; namely, $\mathbf{V}_S = b\mathbf{V}_a$. The regression technique provided estimates of b along with the a_{ij}'s and $\mathbf{U}_G$. Three models were investigated. For case 1 the a_{ij}'s were constrained just as in case 2 of the quadratic theory. The second imposed the case 3 constraint, and the last considered just Stokes drift, i.e., $a_{ij} = 0$.

The prescription of the averaging interval is a delicate balance between two factors. If the averaging period is too short, the number of data points is not much more than the number of parameters and there is the risk that predictive capability will be artificially enhanced. On the other hand, if the averaging period is too long, nonstationary and spatial-scale effects become a problem. Consequently, the question of appropriate averaging periods was investigated in some detail. For this data set it was found that tests of the three basic hypotheses which used statistics from averaging periods ranging from 5 to 21 days yielded the same conclusions with only minor variations in the significance levels.

Each of the models described above were subjected to four types of tests. The first determined the levels of significance of the variance that each of the models explained. Then they were tested for homogeneity of the data base. This was accomplished by testing the differences of regression coefficients for each (nonoverlapping) averaging period with the combined regression coefficients. The third test determined the "best" special case for each theory. Finally, a subjective comparison was made of the best special cases of the three different theories.

In the analysis described above, the drifters move continuously, whereas the FNWC surface wind analysis prescribes the wind on a 2.5° × 2.5° grid every synoptic period. It is necessary then to obtain records of the wind field and drifter velocities at the same point in time and space. A two-step procedure accomplished this. First, from the time series of locations, the drifter position at each synoptic period was interpolated by spline functions. These functions also produced smooth estimates of the drifter velocity. Second, at each synoptic period the wind components were interpolated to the drifter positions by passing a plane through the nearest grid points. In summary, the drifter positions and velocities were interpolated to each synoptic period and then the wind field was interpolated to each drifter. In essence this procedure applies a space and time filter to the drifter data which is roughly comparable to that used in obtaining the wind field.

4. Test of theories

a. Quadratic theory

Typically an analysis of variance partitions the total variance into the sum of the model variance and a residual or unexplained variance. A common measure of the goodness of fit is the ratio of the explained or model variance to the variance R^2 of the observations. Plots of this for each of the three cases for the quadratic theory for the longest record (ID 1173) are given in Fig. 4. The calculations were performed as a type of running average. For a specified day and averaging period the least-squares analysis was centered on that day. For the next time period a new analysis was performed. This pro-

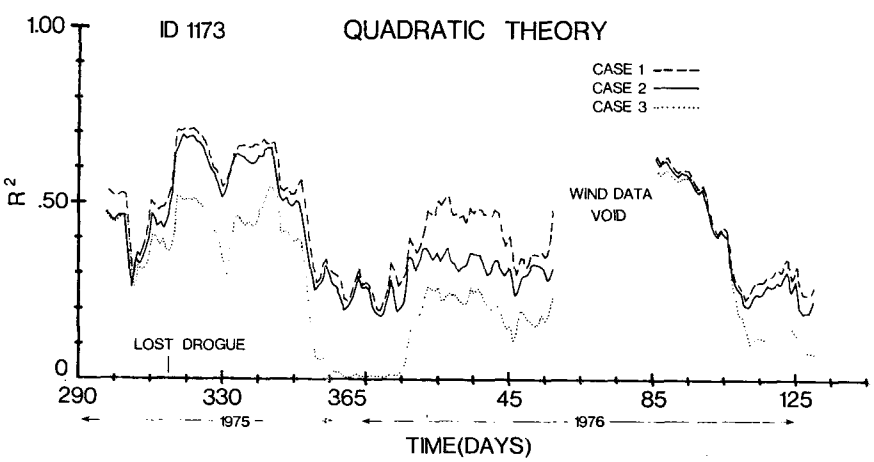

FIG. 4. Ratio of model variances to observed variance R^2 for each case of the quadratic theory for the 21-day averages. The gap in the record is the result of missing wind data at FNWC.

TABLE 1. Average R^2 for quadratic law models for 5-day and 21-day averages

	Case 1		Case 2		Case 3	
ID	5 day	21 day	5 day	21 day	5 day	21 day
1102	0.5414	0.4342	0.4375	0.3924	0.3002	0.2780
1173	0.5026	0.4441	0.3903	0.3988	0.2684	0.2778
1204	0.5482	0.4096	0.4456	0.3679	0.3017	0.2532
1232	0.5331	0.4652	0.4237	0.4493	0.2833	0.2944
1243	0.5764	0.5130	0.4900	0.4964	0.3497	0.3849
1275	0.4420	0.3307	0.3373	0.3036	0.2291	0.2468

Case 1 is the general case. Each of the a_{ij}'s is independent.
Case 2 is the generalized Ekman case. Here $a_{11} = a_{22}$, $a_{12} = -a_{21}$.
Case 3 is the simple Ekman case. Here $a_{11} = a_{12} = a_{22} = -a_{21}$.

cedure gave a running record in time of the model statistics. As explained below this procedure also allowed an evaluation of the homogeneity of the data to be made.

Except for the record lengths, plots of R^2 for the other drifters are very similar; however, values for ID 1275 are somewhat lower than the others. Table 1 summarizes the average R^2 for the entire record for each drifter.

The first test of the model determines the probability that these R^2's are due to chance. This is addressed by testing the null hypothesis H:$a_{ij} = 0$ against not H, by the F distribution. The degrees of freedom are $N - q - 1$ and q, where N is the number of observations and q the number of independent a_{ij}'s. For the 5-day and 21-day averaging periods N is, respectively, 20 and 84. For cases 1, 2 and 3, q is, respectively, 4, 2 and 1.

We first consider the 5-day averages. It is found that H could be rejected with only a 5% chance of error if $R^2 \geq 0.45$, 0.30 and 0.20 for any 5-day average for the first, second and third cases, respectively. Except for case 1 for drifter 1275, R^2's exceed these critical values for well over half the record. For the 21-day averages, any value of $R^2 \geq 0.2$ is significant at the 1% level for all three cases. Only case 3 had any periods where R^2 was less than this critical value. Thus for most of the 5-day and 21-day averaging periods the R^2's are significant. The only exception is the period 355/75 to 20/76. A comparable decrease in R^2 was observed for all active drifters during that time. Here the level of significance of the results was reduced considerably. We have no explanation for this decrease. Nevertheless this period was included in the combined and overall averages.

The next concern is the homogeneity of the data base. Following Williams (1959) this was tested by comparing the regression coefficients from case 1 for each nonoverlapping 21-day averaging period with that obtained from a combined or overall regression. These coefficients were tested by generalized Students' t. In the analysis of the variance the degrees of freedom for the combined regression is 4 (the number of coefficients), for the differences of regression they are $4(m - 1)$, and for the combined residual they are $N - 3m$. Here m is the number of nonoverlapping averaging periods. It is basically the greatest integer in the record length in days divided by the averaging period.

It was found that the differences of the within group and overall coefficients was not significant at the 85% or higher level for all drifters except 1275 where the significance level was about 75%. The significance levels would be considerably higher if the period 355/75–20/76 was not included in the analysis. This means that the data from any particular averaging period are not significantly different at these levels. Thus, the results from any particular averaging period are a reasonable representation of the entire record.

Considering the 21-day cases, Table 1 shows that case 2, where the data specify the angle and one drag coefficient, explains 90% of the variance of the first case. However, the third case, in which the angle between the wind drift current and the wind is fixed at 45°, explains just over 60%. For the 5-day cases, the respective percentages are 80 and 53.

The question of whether the last two cases explain an adequate portion of the first case is addressed as follows: For case 2 the null hypothesis H: $a_{11} = a_{22}$, $a_{12} = -a_{21}$ is tested against not H by an F statistic. Specifically, F is given by

$$F_2 = (R_1^2 - R_2^2)(N - 5)/2(1 - R_1^2), \quad (9)$$

with degrees of freedom of 2 and $N - 5$. The subscripts refer to the appropriate case. Calculated F values for the 5-day and 21-day periods were all less than 1.7 and 3.2, respectively. In order to minimize the chance of a type II error (accepting a false hypothesis) H should be tested at its lowest level of significance. It is found that H cannot be rejected for any drifter at a probability level greater than 80% and 90% for the respective averaging periods.

The test for case 3 proceeds in the same manner except that (9) is replaced by

$$F_3 = (R_1^2 - R_3^2)(N - 5)/3(1 - R_1^2). \quad (10)$$

The degrees of freedom are 3 and $N - 5$. For this case the null hypothesis is H: $a_{11} = a_{12}, a_{22} = -a_{21}$. The values of F_3 range from 1.9 to 2.7 for the 5-day averages and 3.3 to 8.4 for the 21-day averages. Since these values are higher than the previous case there is a risk of a type I error (rejecting a true hypothesis) here. This is minimized by testing H at a high level of significance. For the 21-day averages, H is rejected at the 99% level for every drifter

except 1275 where the significance level is 95%. For the 5-day averages, H is rejected at the 90% level except 1275 where the significance level is 80%.

To summarize the results of these tests on the quadratic theory it was concluded that each of the models explained a significant portion of the variance, the data set was relatively homogenous and that case 2 was the best special case. It explained nearly as much variance as the general case but with two less parameters.

Table 2 summarizes the combined average angle between the surface wind and the model wind drift component for case 2 for ID 1173 as well as

$$\gamma = (a_{11}^2 + a_{12}^2)^{1/2} = \rho_a C_D (2/\rho_w K f)^{1/2}$$

for case 2 for each drifter. The angle is of the order of 15° *cum sole* and the γ values are within the range given by accepted values of drag coefficient C_D and vertical eddy viscosity K.

TABLE 2. Average angle between wind drift and wind and the drag coefficient for the quadratic case 2 for 5-day and 21-day averages.

	Angle (deg)		$\gamma \times 10^{-3}$	
ID	5 day	21 day	5 day	21 day
1102	−11.4	−14.1	0.95	0.81
1173	−9.4	−8.8	0.86	0.76
1204	−13.0	−10.2	1.39	0.91
1232	−11.9	−6.4	0.91	0.85
1243	−12.7	−17.8	0.92	0.86
1275	−22.2	−24.8	1.22	0.97

b. Linear theories

Fig. 5 is a plot of R^2 for ID 1173 for the linear theory and Table 3 summarizes the average R^2's for the different drifters. The conclusions reached concerning the averaging period, the homogeneity of the data and the selection of the best model (case 2) are the same as in the quadratic theory. Table 4 lists the average angle and $(a_{11}^2 + a_{12}^2)^{1/2}$ for the second case for each drifter. As before, it is seen that the angle is of the order of 15°. The scalar coefficient is within the range given in Madsen's study and is considerably less than the value we used in attempting to correct for the wind drag on the buoy.

Comparing the linear and quadratic theories, note that the R^2's for the former theory are all greater than corresponding values from the latter theory. Although the differences are not large we feel, particularly in view of the uncertainties in the observations, that they are sufficient to justify selecting the linear theory as the better representation of the data.

c. Tests of Ekman plus Stokes drift theory

Fig. 6 shows the variance ratio for ID 1173 for the three cases of this theory, and Table 5 lists the average R^2's. Previous conclusions about the data set are valid here also. The F tests show that the hypothesis H: $a_{11} = a_{12} = a_{22} = -a_{21}$ cannot be rejected until the significance level is dropped to 80% for both averaging periods. On the other hand, at the 95% significance level, the hypothesis that all a_{ij}'s are zero is rejected for the 21-day averages. Thus, the classic Ekman wind drift superposed with a Stokes drift component is the best case for this theory.

Table 6 shows the combined average angle for the first case. It is considerably greater than that given in the previous model studies. This points out a fundamental difficulty in comparing Eulerian and Lagrangian measurements of the surface current response to the wind. As the Stokes component is not present in Eulerian data, the angle between the

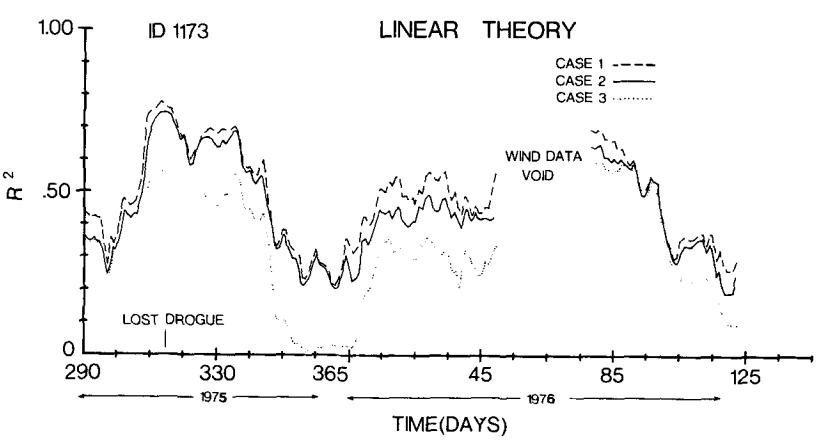

FIG. 5. Ratio of model variances to observed variance R^2 for each case of the linear theory for the 21-day averages. The gap in the record is the result of missing wind data at FNWC.

TABLE 3. Average R^2 for linear law models for 5-day and 21-day averages.

	Case 1		Case 2		Case 3	
ID	5 day	21 day	5 day	21 day	5 day	21 day
1102	0.5761	0.4700	0.4721	0.4298	0.3305	0.3120
1173	0.5361	0.4845	0.4174	0.4449	0.2985	0.3247
1204	0.5905	0.4741	0.4839	0.4414	0.3407	0.3105
1232	0.5632	0.5085	0.4536	0.4905	0.3078	0.3284
1243	0.6014	0.5694	0.5088	0.5467	0.3677	0.4333
1275	0.4896	0.3877	0.3860	0.3643	0.2770	0.3090

Case 1 is the general case. Each of the a_{ij}'s is independent.
Case 2 is the generalized Ekman case. Here $a_{11} = a_{22}$, $a_{12} = -a_{21}$.
Case 3 is the simple Ekman case. Here $a_{11} = a_{12} = a_{22} = -a_{21}$.

wind and wind drift current in that system will be greater than that seen in the Lagrangian system.

Table 6 also lists the b's for case 2. The values are considerably less than the theoretical value of 0.0158. However, there is no angular spreading in this model. There is some evidence (Barnett and Kenyon, 1975) that the spreading function obeys a $\cos^2$ law. Taking this into account reduces the theoretical value to 0.0134, still larger than the observed. Errors in the wind field will cause the least-squares estimates of b to be low. But until these error variances are established it is impossible to say if the discrepancy is the result of experimental error.

Comparison of the Ekman plus Stokes theory case 2 with case 2 of the linear theory indicates no significant difference; i.e., a simple Ekman model with a Stokes drift component explains the observations as well as the two-parameter linear model.

5. Geostrophic calculations

In addition to establishing a model for predicting the wind-induced currents, the procedure adopted here also produces the surface geostrophic velocity. The stick diagram (Fig. 3) shows these for the Ekman plus Stokes case. The combined average U_g and V_g are given in Table 7. It is very encouraging to find that the zonal component is of the order of 0.03 m s^{-1}, in excellent agreement with the mean annual dynamic topography (Wyrtki, 1975; Reid and Arthur, 1975). Except for ID 1275, there is a small southerly component to the surface geostrophic flow. This component is not inconsistent with southerly flow at the eastern end of the subtropical gyre.

Fig. 3 also shows evidence of a 20-day fluctuation in the geostrophic velocity. Similar fluctuations in this region have been associated with baroclinic mesoscale structures (Roden, 1977; Royer, 1978; Kirwan *et al.*, 1978b).

TABLE 4. Average angle between wind drift and wind and the drag coefficient for the linear case 2 for 5-day and 21-day averages.

	Angle (deg)		$(a_{11}^2 + a_{12}^2)^{1/2} \times 10$	
ID	5 day	21 day	5 day	21 day
1102	−12.1	−16.2	0.13	0.12
1173	−13.2	−12.3	0.12	0.13
1204	−14.4	−12.0	0.16	0.15
1232	−12.2	−7.8	0.13	0.14
1243	−15.6	−19.1	0.12	0.13
1275	−26.5	−26.3	0.14	0.13

6. Discussion

a. Linear and quadratic theories

In regard to the tests of the linear and quadratic theories, the results of this study support the following conclusions:

1) The two-parameter, or second cases, are the

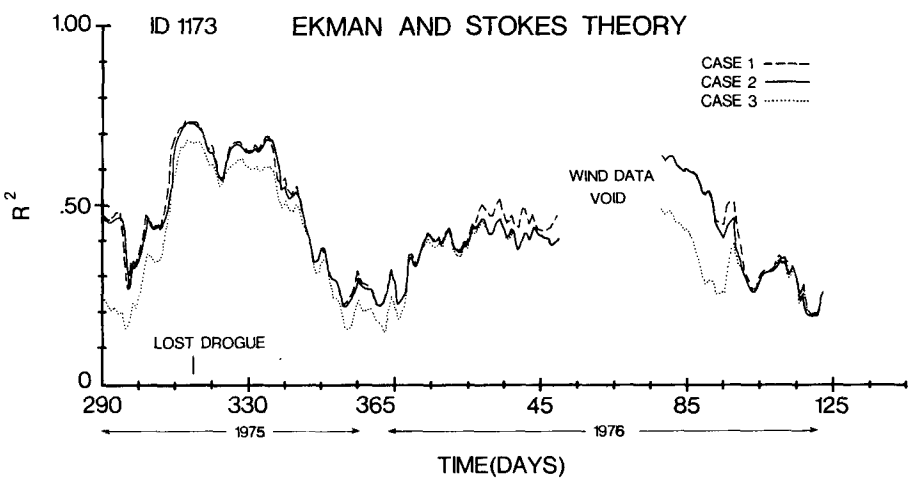

FIG. 6. Ratio of model variances to observed variance R^2 for each case of the Ekman plus Stokes theory. The gap in the record is the result of missing wind data at FNWC.

TABLE 5. Average R^2's for Ekman plus Stokes models for 5-day and 21-day averages.

	Case 1		Case 2		Case 3	
ID	5 day	21 day	5 day	21 day	5 day	21 day
1102	0.4922	0.4294	0.4640	0.4232	0.3189	0.3916
1173	0.4526	0.4541	0.4171	0.4414	0.3352	0.3842
1204	0.5159	0.4552	0.4745	0.4349	0.3948	0.4112
1232	0.4922	0.5025	0.4576	0.4911	0.3612	0.4635
1243	0.5501	0.5575	0.5239	0.5409	0.3738	0.4840
1275	0.4096	0.3607	0.3625	0.3383	0.3192	0.2919

Case 1 is general Ekman plus Stokes drift. Here $a_{11} = a_{22}$, $a_{12} = -a_{21}$.

Case 2 is simple Ekman plus Stokes drift. Here $a_{11} = a_{12} = a_{22} = -a_{21}$.

Case 3 is only Stokes drift. Here $a_{11} = a_{12} = a_{22} = a_{12} = 0$.

most realistic. They explain nearly as much variance as the general cases but with two less parameters.

2) In comparing the linear and quadratic theories, it is clear that the linear theory is best.

3) The angles predicted by the general Ekman models are of the order of 15° and are in good agreement with the findings of Madsen (1977).

Thus, hypotheses 1 and 2 given in the introduction are rejected if Stokes drift is neglected.

b. Ekman plus Stokes

The Ekman plus Stokes model calculations showed that case 2 worked as well as case 1. Moreover, the R^2's for the second case were indistinguishable from the linear case 2. There seems little doubt then that in the Lagrangian system there is a component of flow in the direction of the wind. How much of this is Stokes drift and how much is wind drag on the buoy is moot. In any event, windage is less than half that predicted.

This experiment, then, is insufficient to accept or reject hypothesis 3. Resolution of this issue will, no doubt, require better knowledge of the wind field, more detailed engineering studies of the drifter response to waves and wind than were available to us, as well as Eulerian measurements.

TABLE 6. Average angle between wind drift and wind for Ekman plus Stokes drift case 1 and Stokes coefficient (b) for case 2 for 5-day and 21-day averages.

	Angle (deg)		Stokes coefficient	
ID	5 day	21 day	5 day	21 day
1102	−51.0	−74.6	0.0087	0.0093
1173	−32.3	−65.2	0.0079	0.0096
1204	−31.9	−84.2	0.0114	0.0129
1232	−49.0	−35.6	0.0096	0.0115
1243	−59.6	−139.7	0.0081	0.0090
1273	−44.8	−116.2	0.0065	0.0078

TABLE 7. Geostrophic components—simple Ekman plus Stokes case—21-day average.

ID	U_G (m s^{-1})	V_G (m s^{-1})
1102	0.03	−0.009
1173	0.05	−0.02
1204	0.02	−0.05
1232	0.03	−0.01
1243	0.02	−0.005
1275	0.03	0.02

c. Geostrophic currents

The geostrophic velocities obtained from either Ekman plus Stokes or linear case 2 models are in excellent agreement with that calculated from the mean annual dynamic topography. This means that in order to obtain the geostrophic component from drifter velocity records it is necessary to evaluate the wind drift component as well.

d. Overall

It is encouraging that the results obtained here are in such good agreement with more tightly controlled smaller scale experiments, especially when one considers the crudeness of our data set. When the experiment was conceived this type of analysis was not considered feasible.

Acknowledgments. This research was supported by Contracts N0015-75-C-1052 and N0014-75-C-0537 with the Office of Naval Research at the University of California at San Diego and Texas A&M University, respectively. We thank the crew of the R/V *Thompson* (University of Washington) for their assistance in the drifter deployment.

REFERENCES

Barnett, T. P., and K. E. Kenyon, 1975: Recent advances in the study of wind waves. *Rep. Prog. Phys.*, **38**, 667–729.

Chang, M.-S., 1969: Mass transport in deep-water long-crested random gravity waves. *J. Geophys. Res.*, **74**, 1515–1536.

Davis, R., T. P. Barnett and C. S. Cox, 1978: Variability of near-surface currents observed during the Pole experiment. *J. Phys. Oceanogr.*, **8**, 290–301.

Ekman, V. W., 1905: On the influence of the earth's rotation on ocean currents. *Ark. Mat. Astron. Fys.*, **2**, 1–53.

Friehe, C. A., and S. E. Pazan, 1978: Performance of an air-sea interaction buoy. *J. Appl. Meteor.*, **17**, 1488–1497.

Hasselmann, K., 1970: Wave-driven inertial oscillations. *Geophys. Fluid Dyn.*, **1**, 463–502.

Ianniello, J. P. and R. W. Garvine, 1975: Stokes transport by gravity waves for application to circulation models. *J. Phys. Oceanogr.*, **5**, 47–50.

Kenyon, K. E., 1969: Stokes drift for random gravity waves. *J. Geophys. Res.*, **74**, 6991–6994.

Kirwan, A. D., Jr., G. McNally and J. Coehlo, 1976: Gulf stream kinematics inferred from a satellite-tracked drifter. *J. Phys. Oceanogr.*, **6**, 750–755.

——, and M.-S. Chang, 1978: Effect of sampling rate and random position error on analysis of drifter data. *J. Phys. Oceanogr.*, **9**, 382–387.

——, G. McNally, and S. Pazan, 1978a: Wind drag and relative separations of undrogued drifters. *J. Phys. Oceanogr.*, **8**, 1146–1150.

——, G. J. McNally, E. Reyna, and W. J. Merrell, Jr., 1978b: The near surface circulation of the eastern North Pacific. *J. Phys. Oceanogr.*, **8**, 937–945.

——, G. McNally, M.-S. Chang and R. Molinari, 1975: The effect of wind and surface currents on drifters. *J. Phys. Oceanogr.*, **5**, 361–368.

Lange, P., and H. Hühnerfuss, 1978: Drift response of monomolecular slicks to wave and wind action. *J. Phys. Oceanogr.*, **8**, 142–150.

Longuet-Higgins, M. S., 1969: On the transport of mass by time varying ocean currents. *Deep-Sea Res.*, **16**, 431–447.

Madsen, O. S., 1977: A realistic model of wind-induced Ekman boundary layer. *J. Phys. Oceanogr.*, **7**, 248–255.

Neumann, G. and W. J. Pierson, 1966: *Principles of Physical Oceanography*. Prentice-Hall, 545 pp.

Pierson, W. J., Jr. and L. Moskowitz, 1964: A proposed spectral form for fully developed wind seas based on the similarity theory of S. A. Kitaigorodskii. *J. Geophys. Res.*, **69**, 5181–5190.

Reid, J. L., and R. S. Arthur, 1975: Interpretation of maps of geopotential anomaly for the deep Pacific Ocean. *J. Mar. Res.*, **33** (Suppl), 37–52.

Roden, G. I., 1977: On long-wave disturbances of dynamic height in the North Pacific. *J. Phys. Oceanogr.*, **7**, 41–49.

Royer, T. C., 1978: Ocean eddies generated by seamounts in the North Pacific. *Science*, **199**, 1063–1064.

Williams, E. J., 1959: *Regression Analysis*. Wiley, 214 pp.

Wyrtki, K., 1975: Fluctuations of the dynamic topography in the Pacific Ocean. *J. Phys. Oceanogr.*, **5**, 450–459.